Cu-DOPED ZnTe THIN FILMS FOR POTENTIAL ENERGY APPLICATIONS

W. A. SYED[a,*], S. AHMED[a], M.S. SALEEM[a], N. A. SHAH[b]
[a]*Department of Physics, International Islamic University, Islamabad, Pakistan, 45320*
[b]*Department of Physics, COMSATS Institute of Information. Technology, Islamabad 45320, Pakistan*

Thin films of Zinc Telluride (ZnTe) were deposited on the corning glass by the two source evaporation method. The annealing was carried out 300°C at a vacuum of 10^{-3} mbar for about an hour. The effect of varying thickness and doping of copper on the physical properties of ZnTe thin film has been investigated. The structural properties including crystallite size, microstrain and dislocation density were determined by X-ray diffraction (XRD) and surface morphology and grain size by scanning electron microscopy. The UV-VIS-NIR spectrophotometery was carried out to investigate optical transmittance, which was decreased from 98% to 60% with increasing thickness 129 to 1514 nm. The electrical properties were determined by mean of Hall Measurement system and resistivityand mobility was calculated. The aim of Cu doping was to investigate the effects of reduced resistivity on electrical properties of ZnTe thin films and the potential uses as back contact for CdTe in CdTe/CdS heterojunction solar cells.

(Received February 23, 2015; Accepted May 1, 2015)

Keywords: ZnTe, Thermal evaporation, structural properties, Electrical and optical properties, Solar cell

1. Introduction

ZnTe is one of the interesting materials for potential photovoltaic applications in particular with solar cells, photodiodes and LED. Because of its excellent features including large energy band gap, low resistivity and high visible range transparency ZnTe is used in variety of microelectronic and optoelectronic devices [1–4].ZnTe has been extensively studied for the applications in green light emitting diode and as back contact material for CdTe in CdTe/CdS heterojunction solar cells [5-6].ZnTe is used as a substrate for the growth of CdTe and the heterostructures based on ZnTe and HgTe used for infrared optics [7]. ZnTe is famous for its use in photodetectors, quantum well structures [8-9], tandem solar cells and terahertz (THz) signal generation and detection [10-11]. The use of ZnTe, usually a p-type semiconductor material, instead of n-type layer (CdS) as wide band gap window produces higher potential barriers for electron transport yielding higher value of V_{oc}. The use of ZnTe as a window layer in solar cells also reduces the toxic nature by replacing chemical bath deposited CdS layers in currently developed thin film solar cells [12].

A number of techniques have been used to prepare ZnTe thin film including chemical vapor deposition [13-14], electrochemical deposition [15], molecular beam epitaxy [16], hot wall epitaxy [17], and pulsed laser deposition [18]. It was observed that the deposited films have cubic zinc blende structure [19-23].Recently, due to significant applications in the micro and optoelectronics, the study of copper doped zinc telluride thin film has become very interesting for the research community [24].

[*]Corresponding author: adil.syed@iiu.edu.pk

In the present investigation, ZnTe thin film was prepared by two source evaporation method and the effects of varying thickness, Cu doping and annealing on the physical properties were investigated and reported.

2. Experimental

Zinc telluride thin films were deposited by two source thermal evaporation technique on corning glass (7059) substrate. The glass substrate were cleaned with isopropyl alcohol (IPA) in an ultrasonic bath, and placed in the substrate holder. Zinc and tellurium (99.99% pure) were used as source element for the deposition. The chemical reaction follows the equation as under

$$ZnTe \longleftrightarrow Zn + Te \tag{1}$$

The material was placed in two graphite crucibles at a distance of 3 cm apart; with ahole of adiameter of 2 mm on the top of point source. Both crucibleswereindependently heated by 500 W quartz lamps and K-type thermocouples was inserted into the graphite crucibles fixed in E306A vacuum coating system as a temperature controllers. The glass substrate was heated by infrared (IR) heater, while the evaporation rate was controlled with quartz crystal FTM3 thickness monitor. During evaporation, 12 cm distance was fixed between the substrate and source material. The source temperature of Zn and Te were fixed at 540^{o}Cand 480^{o}C respectively witha constant substrate temperature at 400^{o}C. The pressure of the chamber was kept at 10^{-6} mbar during the experiment.

Copper was doped to enhance the electrical properties of the fabricated ZnTe thin films by ion-exchange method. The thin films were dipped into the solution of $Cu(NO_3)_2$ and distilled water with a ratio of 0.2 g: 200 ml (0.533 moles/L). Different concentration of copper was achieved in ZnTe films with different ranges of dipping time from 5-20 minutes into the $Cu(NO_3)_2$ solution. The samples were dried in a closed clean glass desiccators and annealed at 300^{o}C at vacuum of 10^{-3} mbar for an hour. The structural, morphological, optical and electrical analysis was carried out with the help of JEOL X-ray diffractometer, scanning electron microscopy, Perkin Elmer spectrophotometer LAMBDA 950 and Hall measurement system Ecopia HMS 3000 respectively.

3. Results and discussion

3.1 Structural Analysis

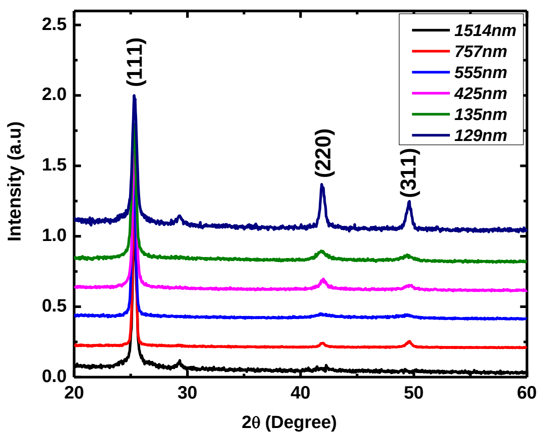

Fig. 1. XRD patterns of as-deposited thin films of various thicknesses.

Table 1. XRD measurements; Variation of crystalline size and microstrain with varying thickness of ZnTe film.

Film thickness (nm)	**Crystallite Size D (Å)**	**Dislocation density (ρ) lines/ min^2 (10^{+15})**	**Microstrain ϵ(10^{-3})**	**d_0(Å) d/(1-ϵ)**	**Δd (Å) (10^{-3})**
1514	216.357	2.136	1.507	3.522	5.30
757	240.399	1.730	1.675	3.515	5.88
555	197.077	2.574	1.674	3.521	5.89
425	214.339	2.136	1.838	3.530	6.49
135	240.352	1.731	1.842	3.526	6.49
129	196.641	2.586	1.70	3.517	5.89

The X-ray diffraction system uses CuK_α radiation source, which has wavelength 1.5418 Å. Figure 1 shows the thickness dependent XRD patterns of as deposited thin films. The main peak of all the samples is found at similar position and can be listed as cubic ZnTe lattice. The prominent (111) peak has been used to calculate the lattice constant. With the help of Scherer's formula the average grain diameter D(Å) has been determined [25].

$$D(\text{Å}) = k\,\lambda(\text{Å})/(L\cos\theta) \tag{2}$$

Where k is the Scherer's constant and equal to 0.94, L is FWHM in radian corresponding to the maximum peak intensity and θ is the Bragg's angle in degrees. The micro strain is calculated as proposed in reference [26]

$$\text{Microstrain} = (L\cos\theta)/4 \tag{3}$$

List of the prepared samples with crystallite size, dislocation density, micro strain and intra-layer spacing are summarized in Table 1. The XRD plots show that the thin films were polycrystalline in nature [27], andthe peaks were matched with the reference cards [28].The variation in lattice constant were measured as 5.30, 5.88, 5.89, 6.49, 6.49 and 5.89 x 10^{-3} Å for the thin films of thicknesses 1514, 757, 555, 425, 135 and 129 nm respectively. The FWHM of the main peak decreases with increasing thickness. This shows a drop in the defects due to shrinking of the grain boundaries. The escalating crystallite size and shrinking dislocation density are due to the reduction in grain boundaries. This process results removal of the defects in the films. The growing micro strain and change in d-spacing (Δd) are probably the reasons for the peaks shifting in the X-ray diffraction spectra. The dislocation density was calculated by the equation

$$\rho = 1/D^2 \tag{4}$$

In Figure 2, XRD pattern of the copper doped sample with 555 nm thickness is presented. The peaks are matched with reference card, and it is found that all the prominent peaks of CuZnTe compound have increasing trends after Cu-doping/content. Table 2 shows the structural parameters of sample with 555 nm measured by XRD with different doping time.

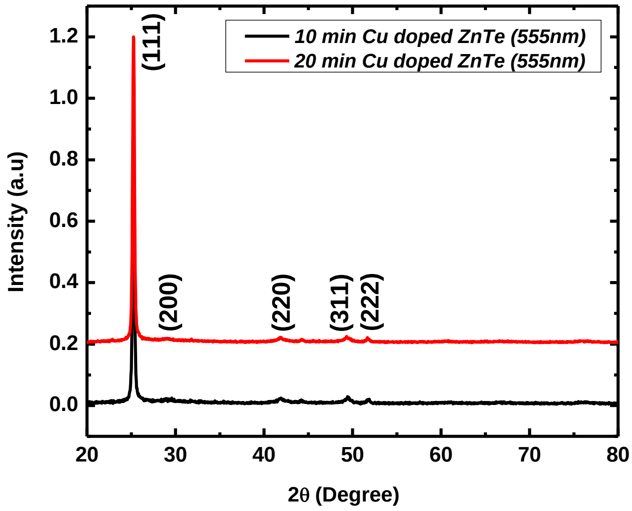

Fig. 2. XRD results of Cu doped ZnTe (555 nm) thin film.

Table 2 Variation in d-spacing, crystallite size, dislocation density and microstrain in 555 nm film with Cu doping time.

Sample	**FWHM (deg)**	**d-Spacing**	**Crystallite size (Å)**	**Dislocation Density (ρ) lines/min^2(10^{+15})**	**Micro strain 10^{-3}**
as-deposited	0.432	3.523	197.077	2.574	1.838
10 min Cu doping	0.442	3.521	192.619	2.695	1.881
20 min Cu doping	0.452	3.513	188.357	2.818	1.923

3.2 Surface morphology

Scanning electron microscopy (SEM) was used to obtain micrographs of as-deposited ZnTe thin films at magnification of 50,000 and shown in Figure 3. Each sample has a consistent grain size however the grain sizes varies for different sample. Voids can be seen randomly, however most of the observed voids were disappeared during the annealing process and this phenomenon is expected to be continued in case of further annealing [29]. Generally, the increasing thickness causes increase in average grain size, as shown inSEM images. It has been found that the thin film grown with higher thicknessesare in better and relaxed mode with less defects and stresses, resulting larger grains. Small amount of defects shows good crystallinity in grown ZnTe thin films [30].

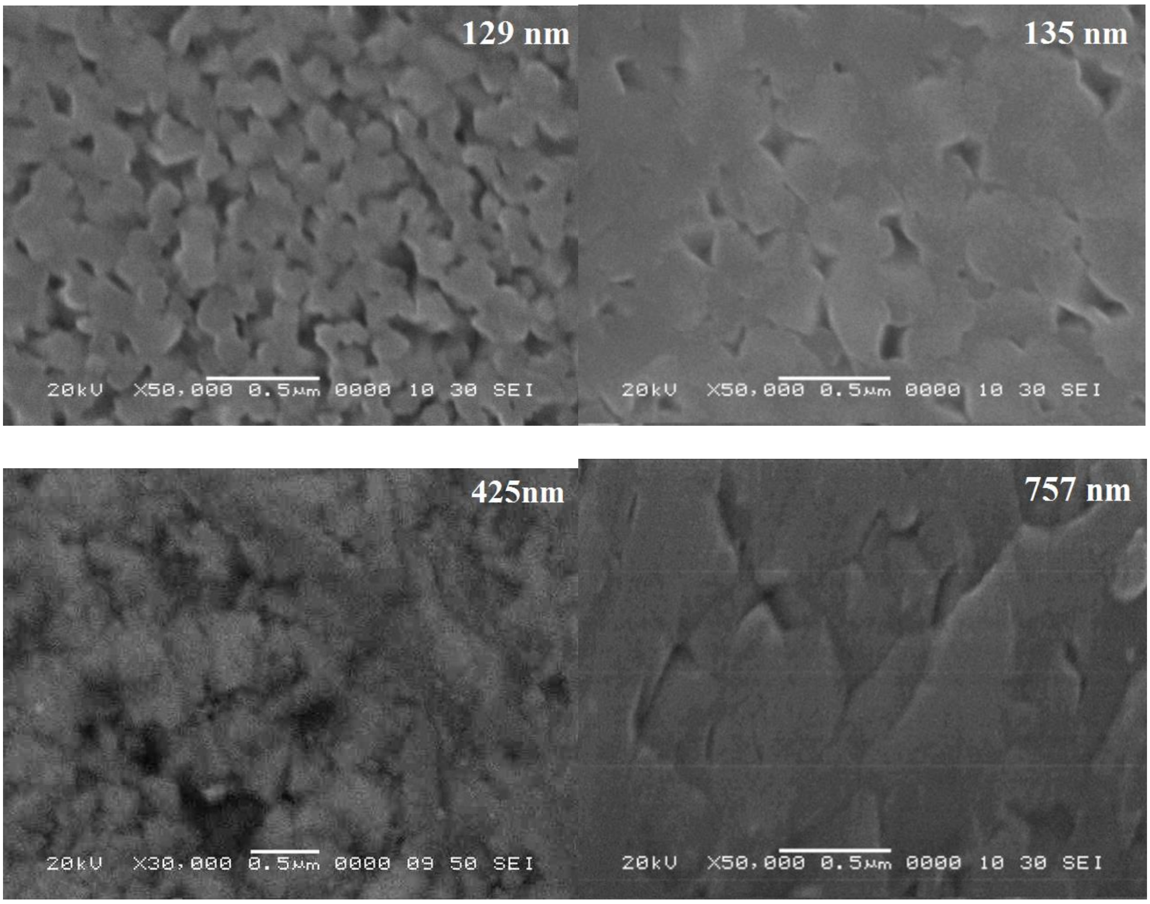

Fig. 3 SEM images of as-deposited ZnTe thin films of various thicknesses.

The SEM micrographs were again obtained for the copper doped sampleswith respective mass percentage of the dopant and presented in Figure 4. The percentage mass composition of the doped material was determined by using Energy Dispersive X-ray (EDX), showing significantly increase grain sizes. The surface of doped sample is not much smooth as compared to that of as deposited sample. It seems that most of copper was concentrated on the surface of the sample.

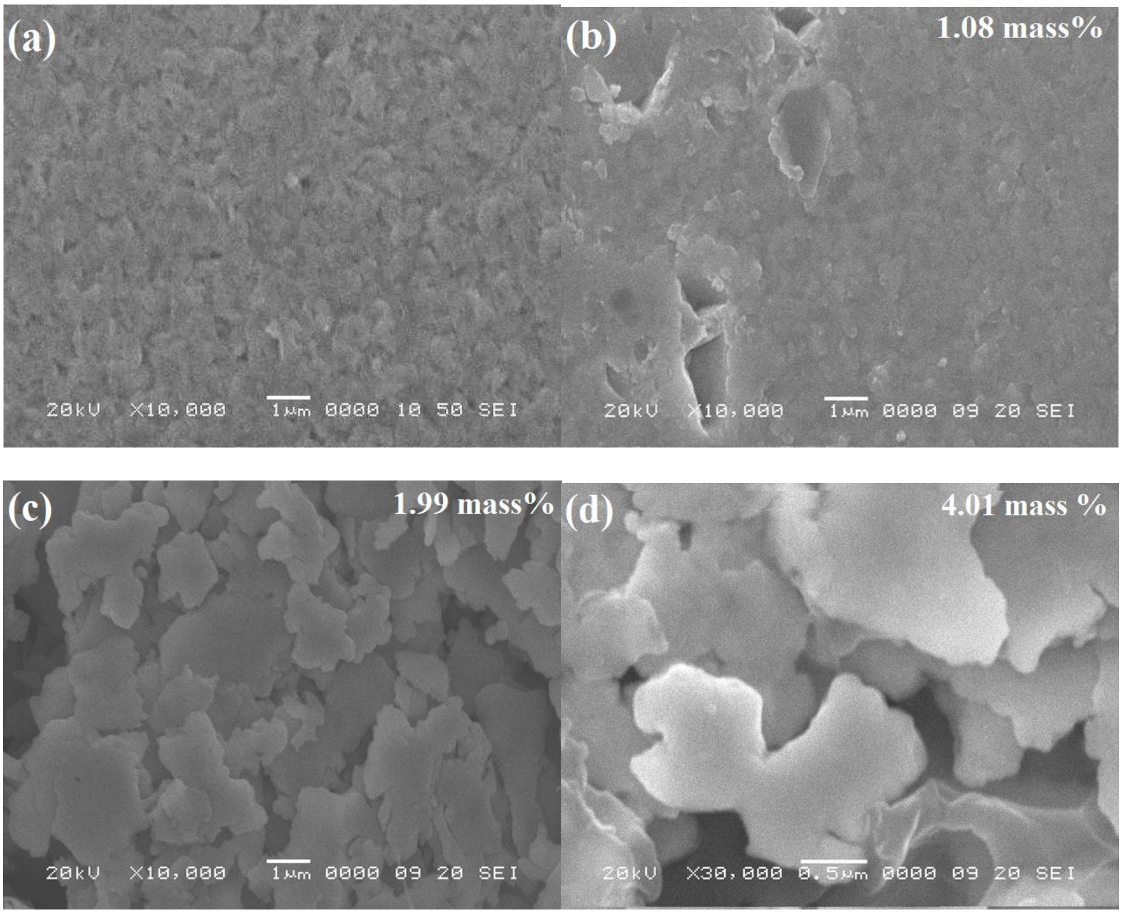

Fig. 4. SEM images of Cu doped 555 nm ZnTe thin films. (a) as-deposited, (b) 5 min doping, (c) 10 min doping, (d) 20 min doping.

3.3 Optical properties

The optical parameters were investigated, which includes refractive index, transmission, absorption coefficient and energy band gap of thin films. The percentage transmittances within the wavelength range of 500-2000 nm of the samples were obtained using UV–VIS-NIR spectrometer. The UV-VIS-NIR spectra are shown in Figure 5. It was found that the increasing thickness causes decrease in the transmission. There is a sharp fall from 98 to 60% in the transmittance as the thickness rises from 129 to 1514 nm; due to increase in the density of the film. Due to highly transparent in visible and IR region, these thin film samples are therefore suitable as window layer in solar cell application [13,31]. The given thickness of the ZnTe thin films was found with the help of Swanepoel model [32]. The optical parameters for one of the sample are given in Table 3. For the energy band gap, in Figure 6, the plots of energy as function of $(\alpha\times \text{energy})^2$ are drawn, where α represents the absorption coefficient. The band gap of the thin films were found in between 2.20 to 2.32 eV and summarized in Table 4. The annealing produced very good effects on the transmittance. The graph of transmission of as-deposited and annealed 555nm thin film is shown in Figure 7. It is evident that the transmission has been significantly increased with the annealing. We take the sample 555 nm and immersed it into copper nitrate solution for different times for doping. Figure 8 shows the transmission behavior of Cu-doped samplesof different immersion times. A decrease in transmission is clearly seen with increase in immersion time for the doped sample. The energy band gap of Cu-doped samples has been shown in Figure 9. Cu introduces additional energy levels in the ZnTe band gap, close to the valence band edge with a consequent reduction of the energy associated with direct transition. Shifting of the optical energy band gap towards the low-energy region is therefore associated with the introduction of the Cu impurity level between the valance and conduction bands [33]. The change in the energy band gap at different immersion times is summarized in Table 5.

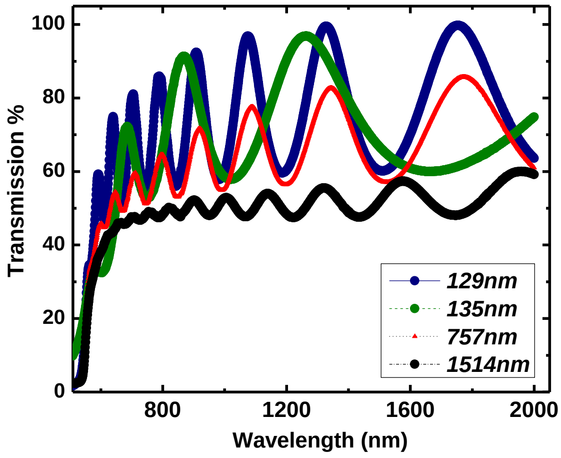

Fig. 5.Plot of transmission curve of ZnTe thin film of various thicknesses.

Table 3 Optical parameters of ZnTe (757nm) thin film.

λ_M (nm)	λ_m (nm)	T_M	T_m	n
601	577	57.88	37.23	2.99
646	610	45.41	44.76	1.63
711	671	59.65	49.23	2.24
795	747	64.64	51.21	2.32
917	846	71.67	53.09	2.43
1089	992	77.62	54.94	2.49
1344	1198	82.74	56.45	2.53
1773	1528	85.76	57.08	2.56

Table 4 Variation of bandgap with thickness ZnTe thin film.

Thickness (nm)	Energy Band gap (eV)
757	2.236
555	2.223
425	2.208
135	2.228
129	2.327

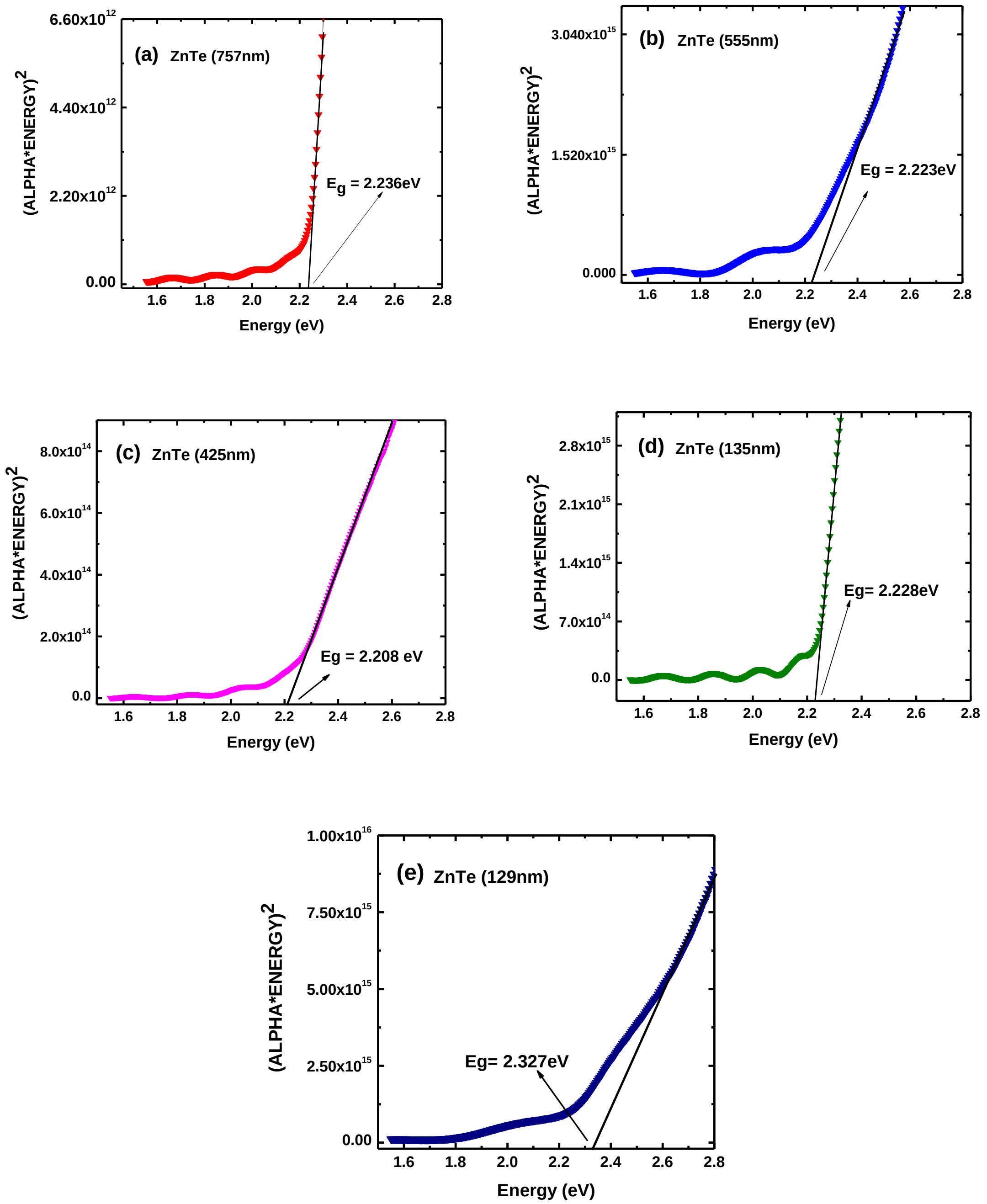

Fig. 6. Band gap Energy of ZnTe thin film of various thicknesses

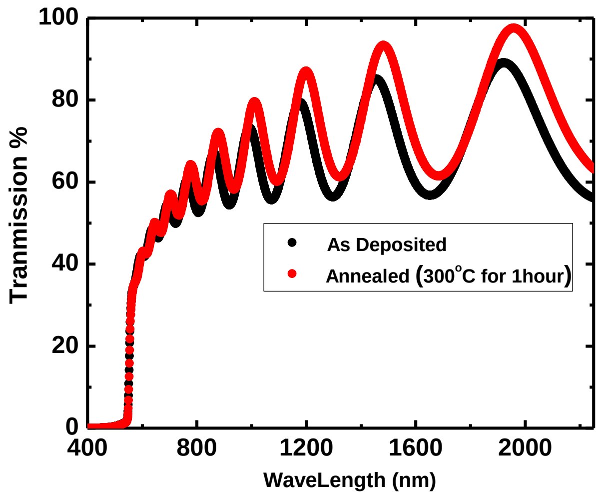

Fig. 7.Plot of transmission curve of as-deposited and annealed ZnTe (555 nm) thin film.

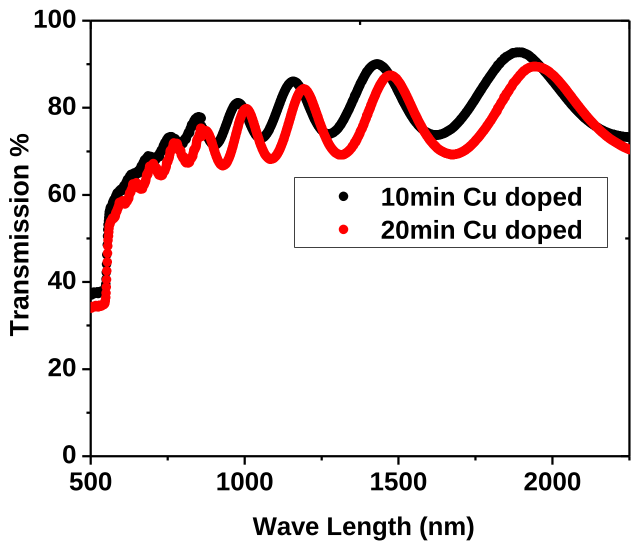

Fig. 8.Comparison between 10min and 20min Cu doped ZnTe (555 nm) thin film.

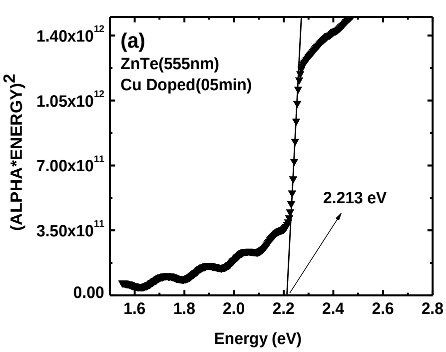

(a)

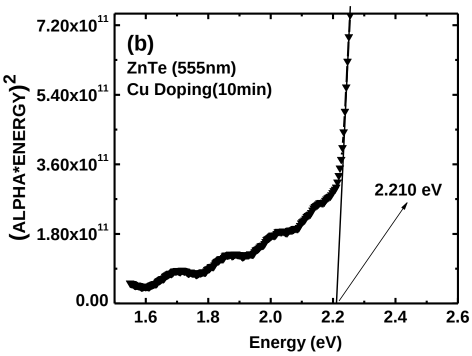

(b)

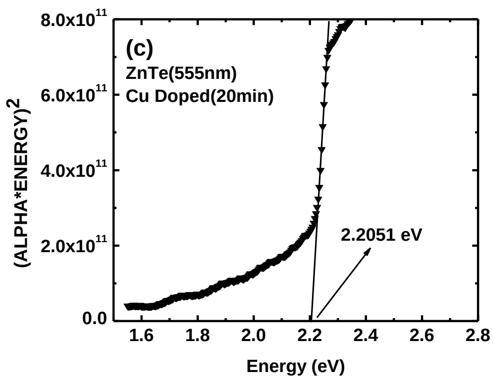

(c)

Fig.9. Band gap energy of Cu doped of 555 nm ZnTe thin film. (a) 5 min doping, (b) 10 min doping, (c) 20 min doping.

Table 5 Variation of bandgap with Cu doped ZnTe thin films.

ZnTe thin film (555 nm)	
Cu-Doping Time (Minutes)	**Energy band gap (eV)**
As-deposited	2.223
5	2.213
10	2.210
20	2.205

3.4 Electrical properties

Electrical resistivity and mobility at room temperature were measured by the Hall effects measurement system. Table 6 shows the changes observed in resistivity and mobility in as deposited and doped samples with respective thicknesses.Increasing thickness of the film causes fall in the resistivityranges from 17.72 x 10^5 to 17.03 x 10^2 ohm-cm. The ultimate change in resistivity is dueto the corresponding grain size [34-35]. With higher grain size, the defects were found decreasing causing decrease in the resistivity.Resistivity measurements showed a drastic reduction, for example in case of 757 nm Cu-doped sample is from 17.03 x 10^2 to 2.12 x 10^2 ohm-cm.

Increasing thickness of samples also causes increase in mobility, which wasincreasedfrom 4.73×10^1 to 54.5×10^1 cm^2/Vs with increasing thickness given in Table 6.

Table 6 Variation of Resistivity & mobility before and after Cu-doping.

Thickness (nm)	**Resistivity (ohm-cm)**		**Mobility (cm^2/Vs)**	
	as-deposited (10^2)	**Cu-doped (20 min) (10^2)**	**as-deposited (10^1)**	**Cu-doped (20 min) (10^1)**
757	17.03	2.12	54.5	61.6
555	202.8	79.8	32.3	76.9
135	7385.0	214	6.11	299.0
129	17720.0	26.7	4.73	165.0

4. Conclusion

ZnTe thin films were prepared by two source thermal evaporation technique. The experimental results show that thin films of ZnTe have cubic zinc blende; the preferred growth orientation was found in (111) direction. On average the crystallite size was increased from 196.64 to 240.39 Å for corresponding thickness from 129 to 757 nm respectively. Crystallite size varied with Cu doping of 20 min from 197.08 to 188.35 Å. With increasing immersion time from 5 to 20 minutes, the composition of copper in the samples were increased from 1.08 to 4.01 mass%. The optical transmission decreases with increasing thickness and higher copper contents. On comparing the as-deposited and Cu doped samples, the energy band gap decreases slightly from 2.22 to 2.20 eV.

The experimental results showed that the as-deposited ZnTe films have high electrical resistivity and decreased with the increase of film thickness and Cu-doping. The electrical resistivity of ZnTe thin films after Cu-doping was dropped to several orders of magnitudewith significant increase in mobility. The important factor is to decrease resistivity of films but not at the cost of transmission so that it can be used efficiently in opto-electronic devices.

References

[1] J. D. Merchant and M. Cocievera, Journal of The Electrochemical Society, **143**, 4054 (1996).
[2] T. Ota and K. Takahashi, Solid-State Electron. **16**, 1089 (1973).
[3] R. Bhargava, (Ed). Properties of Wide Band gap II-VI Semiconductors. Inspec, (1997).
[4] A. Rohatgi, S. A. Ringel, R. Sudharsanan, P.V. Meyers, C.H. Liu, V. Ramanathan, Solar Cells, **27**,219 (1989).
[5] D.L. BaEtzner, R. Wendt, A. Romeo, H. Zogg, A.N. Tiwari, Thin Solid Films. **463**, 361 (2000).
[6]D. Rioux, D.W. Niles, H. Hochst, J. Appl.Phys.**73**(12),8381 (1993).
[7] M. Jain, V. V. Godlevsky, J. J. Derby and J. R. Chelikowsky, Phys. Review B, **65**, 952 (2001).
[8] H. Hamdi, S. Valette, Journal of applied Physics, **51**,4739 (1980).
[9]T. Mahalingam, V.S. John, P.J. Sebastian, Journal of Physics: Condensed Matter, **14,** 5367 (2002).
[10] N. Amer, W.C. Hurlbut, B.J. Norton, Y. S. Lee, T.B. Norris, Applied Physics Letter, **87**,221111 (2005).
[11] M. Walther, F.R. Mark, F.A. Hegmann, Applied Physics Letter, **87**,261107 (2005).
[12] D. G. Diso, F. Fauzi, O. K. Echendu, etal , A. R. Weerasinghe, I. M. Dharmadasa. Journal of Physics: Conference Series **286**,012040 (2011).
[13] W. S. Wang, I. Bhat, Materials Chemistry and Physics.**5**,80 (1997).
[14] U. Pal, Semicond. Sci. Technol. **8**,1331 (1993).

[15]A.E. Rakhshani, Semiconductor Science and Technology.**19**,543 (2004).
[16] M.S. Jang, S.H. Oh, K.H. Lee, J.H. Bahng, J.C. Choi, K.H. Jeong, H.L.Park, D.C. Choo, D.U. Lee, T.W. Kim, Journal of Physics and Chemistry of Solids **64**,357 (2003).
[17] D. Shindo, Y. G. Park, B.J. Kim, J. F. Wang, M. Isshiki, Journal of Physics: Condensed Matter, **14**, 13305 (2002).
[18] S. Bhumia, P. Bhattacharya, D.N. Bose, Materials Letters. **27**,307 (1996).
[19] B. Maiti, P. Gupta, S. Chaudhuri and A. K. Pal, Thin Solid Films, **239**,104 (1994).
[20] T. A. Gessert, X. Li, T. J. Coutts, A. R. Mason and R. J. Matson, Journal of Vacuum Science & Technology A, **12**(4), 1501 (1994).
[21] Michael Neumann-Spallart and Christian Konigstein, Thin Solid Films, **265**, 3 (1995).
[22] Jing-quan Zhang, Liang-huan Feng, Wei Cai, Jia-gui Zheng, Ya-ping Cai, Bing Li, Li-li Wu Ye Shao, Thin Solid Films, **414**, 113 (2002).
[23] T. Mahalingam, V.S. John, G. Ravi and P.J. Sebastian, Cryst. Res. Technol. **37**(4), 329 (2002).
[24] T. Mahalingam, V.S. John, S. Rajendran, P.J. Sebastian, Semiconductor Science and Technology, **17**, 465 (2002).
[25] J. Santamaria, I. Martil, E. Iborra, G.G. Diaz, F.S. Queada, Solar Energy Matter **28**,31 (1990).
[26] S.N.Sahu, S.Chandra, Solar Cells, **22**,163 (1987).
[27] J.W. Orton, B.J. Goldsmith, J.A. Chapman, M.A. Powell, Journal of Applied Physics, **53**,1602 (1982).
[28] JCPDS Card Nos. 01-072-4848, 00-015-0746, 00-015-0746, 01-071-8947, 03-065-0385 and 01-072-4848.
[29] S. M. Salem, M. B.Seddak, A. M Salam, H.A. Salch, Journal of Applied Sciences Research, **7**,698 (2011).
[30] J. Pattar, S.N. Sawant, M. Nagaraja, N. Shashank, K.M. Bala Krishna, G. Sanjeev, H.M.Mahesh, International Journal of Electrochemical Science, **4**, 369 (2009).
[31] V. S. John, T. Mahalingam, Jinn P. Chu, Solid State Electronics **49**,3 (2005).
[32] R. Swanepoel, Journal of Physics E: Scientific Instruments, **16**,1214 (1983).
[33] D.K. Schroder, Semiconductor Material Device Characterization, 2nd ed. New York: Wiley, (1998).
[34] A. K. S. Aqili, A. Maqsood, Z. Ali, Applied Surface Science, **180**,1 (2001).
[35] S.J. Ikhmayies, R.N. Ahmad-Bitar, American Journal of Applied Sciences **5**,1141 (2008).